Physics And Applications Of Josephson Junctions

Nicolas Kahne

14.12.2021

Contents

1 Theoretical Background

1.1 Macroscopic Quantum Model

Quantum mechanical properties are typically only observed at atomic scales. One of those properties is the quantized nature of *microscopic* quantities such as spin or orbital angular momentum of single particles. Macroscopic objects on the other hand are well described by classical mechanics. There are few exceptions to this such as *superconductivity*, where classical laws do not sufficiently describe the phenomenon. The reason for this is that superconductivity is a *macroscopic quantum phenomenon*, meaning its physical quantities are quantized on a macroscopic length scale. The theoretical description for these phenomena was realized by Fritz London within the *macroscopic quantum model*. It states that macroscopic objects (e.g. a bulk superconductor) can be described by a single wavefunction $\psi(\mathbf{r}, t)$. This can be understood by the fact that the charge carriers of the supercurrent are not single electrons but rather electron pairs forming Cooper pairs. These objects carry a spin of 0 and therefore obey Bose-Einstein statistics. At very low temperatures all Cooper pairs can occupy the same ground state, such that their energies and therefore time devolutions of their phases are the same. Also, since the distance between the electrons of one Cooper pair is much larger than the distance between Cooper pairs, their wavefunctions will overlap strongly. This causes a so-called *phase-lock*. These two effects will result in many pairs sharing the same phase, making it a macroscopic quantity. Now the whole ensemble of electrons can be described by a single wavefunction

$$\psi(\mathbf{r}, t) = \psi_0(\mathbf{r}, t)e^{i\theta(\mathbf{r},t)} \tag{1}$$

This allows for a precise description of superconductivity. Furthermore, several *macroscopic quantum phenomena* result from these coherence effects. For instance, superfluidity is a similar phenomenon that describes frictionless flow of liquid helium at very low temperatures. Two important consequences of the macroscopic quantum model are *flux quantization* and the *Josephson effect*, which are crucial to fully understand Josephson junctions. They will be discussed in the following.

1.2 Flux Quantization

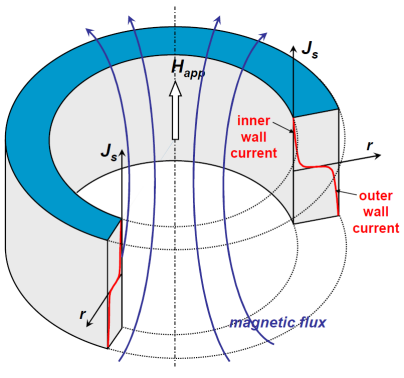

Figure 1: Superconducting cylinder in an external magnetic field.

We start investigating the magnetic flux Φ associated with the superconducting current. The experimental setup is depicted in figure 1. A superconducting cylinder is threaded by an external magnetic field $\vec{H}$ at low temperatures. Since those fields are expelled from superconductors, shielding currents arise at the edges of the cylinder. If the walls are thick compared to the *London penetration depth* λ_L, their center is current-free. Now, the external field is turned off and the shielding currents remain due to the absence of friction. This will result in a trapped flux inside of the cylinder. Since the supercurrent can be described by a single wavefunction ψ, one would expect to observe quantized properties. To determine if this is the case

for the magnetic flux, a loop integral of the current density J_s along the current-free path is performed. This results in

$$\Phi = \frac{h}{q_s} n = \frac{h}{2e} n \equiv \Phi_0 n \ , \tag{2}$$

with the *flux quantum* $\Phi_0 = 2 \cdot 10^{-15}$ Tm^2 and n being an integer number. This means that only n flux quanta will remain trapped inside the cylinder. The flux quantization is a direct consequence of the complex phase being a macroscopic quantity in superconductors and it will play a central role in Josephson junctions and its applications.

1.3 Josephson Effect

The second macroscopic phenomenon is the *Josephson effect*. Here, two identical superconductors S_1 and S_2 are connected via a weak link with an external current source applied, as shown in figure 2a and 2b. In this case a thin insulator is used for the weak link. This configuration is denoted as superconductor-insulator-superconductor (SIS) or Josephson junction. The question is now whether a current flow via tunneling is expected to happen when there is no normal current present. A single e^- has a low tunnel probability, making it seem unlikely for Cooper pairs consisting of two e^- to cross the insulator. However, one has to remember that both e^- are described by the same wavefunction. Therefore, the coherent phase enables the Cooper pair to tunnel as if it were a single e^-, with the same probability.

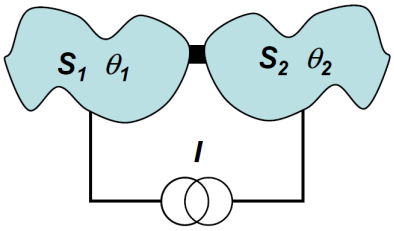

(a) Weakly connected superconductors.

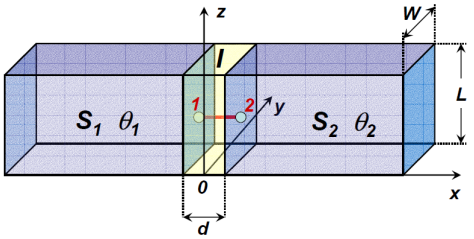

(b) SIS junction, also referred to as a Josephson junction.

Figure 2: Josephson effect leads to current flow through the weak link (insulator).

Brian D. Josephson predicted this effect in 1962 and was experimentally proved one year later by *P. Anderson* and *J. Rowell*.

1.4 Josephson Equations

Analyzing the supercurrent density J_s between both superconductor electrodes, Josephson derived the so-called *Josephson equations*. Assuming J_s to be homogeneous over the junction area and the phase θ varying slowly in the electrodes, he realized that J_s must depend on the phase difference φ. Also, a phase change of 2πn leaves the wave functions $\psi_{1,2}$ unaltered. J_s must

therefore vary sinusoidally with φ. The relation is given by

$$J_s = J_c \sin(\varphi) \tag{3}$$

This is the **1. Josephson equation**, also referred to as the *current-phase relation*. Here, φ is the most general form of the phase difference, meaning it accounts for possible electromagnetic fields inside of the junction:

$$\varphi(\mathbf{r},t) = \theta_2(\mathbf{r},t) - \theta_1(\mathbf{r},t) - \frac{2\pi}{\Phi_0}\int_1^2 \mathbf{A}(\mathbf{r},t)\cdot dl \ , \tag{4}$$

where $\mathbf{A}$ is the vector potential and the integration limits are the edges of the insulating barrier, as depicted in figure 2b.
J_c is the *critical Josephson current density*. It is proportional to the coupling strength of the two electrodes and sets a threshold for the supercurrent:

$$J_c = \frac{4e\kappa n_s}{\hbar} \ , \quad \kappa \coloneqq \text{coupling constant} \ , \quad n_s \coloneqq \text{Cooper pair density} \ . \tag{5}$$

If φ is constant in time the current will be as well. This case will be referred to as the *dc Josephson effect*. Taking the time derivative of φ leads to the **2. Josephson equation**

$$\frac{d\varphi}{dt} = \frac{2\pi}{\Phi_0} V \ . \tag{6}$$

So for a varying phase there is a finite voltage drop across the junction and the current varies sinusoidally. Consequently, this is the *ac Josephson effect*. Both equations define the basis for physics of Josephson junctions, as they will be used to explain the behaviour of currents and voltages in different scenarios.

2 Josephson Junctions

2.1 Zero Voltage State

The dc Josephson effect implies, that current flows across the junction without a voltage drop. This is called the *zero voltage state* and it is only valid, as long as the current doesn't exceed J_c and the temperature is low enough. Otherwise the system would switch into the *voltage state*, which will be addressed in subchapter 2.2.

2.1.1 Extended Junction In An External Magnetic Field

In order to motivate the structure of a *SQUID* (chapter 3), it is reasonable to investigate the behaviour of an extended junction threaded by an applied magnetic field. Extended means the area of the insulator is large enough to assume a spatial dependence of φ and J_s. Figure 3 describes the setup.
Two superconductors S_1 and S_2 are separated by a thin insulator I of thickness d. A dc current source is connected to the electrodes, driving the current in negative x-direction. The plot on

the left shows the strength of the external magnetic field B_y along the x-axis. It is constant inside the insulator and decays exponentially into the electrodes, as superconductors expel magnetic fields depending on the London penetration depth λ_L.

The question is now how exactly does the phase difference and the current density vary along the zy plane. Similar to the flux quantization, the approach is again a loop integral depicted by the red dotted line. The points Q_a, Q_b and P_c, P_d mark two different phase differences along the integration path. The calculation is done by considering the four separate sections divided by the points. Knowing the total phase shift along the closed contour must equal $2\pi n$, the calculation leads to the relation

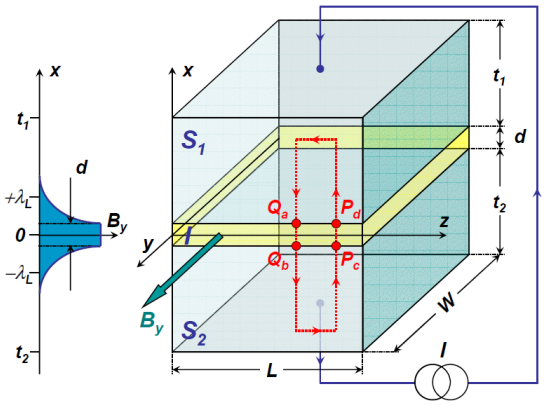

Figure 3: Extended junction connected to a dc current source, threaded by a magnetic field in y-direction.

$$\varphi(z) = \frac{2\pi}{\Phi_0} B_y t_B z + \varphi_0 \ , \tag{7}$$

with $t_B = d + 2\lambda_L$ and φ_0 being the phase difference at $z = 0$. This expression can now be inserted into the 1. Josephson equation (3) to obtain the supercurrent density J_s:

$$J_s(y,z) = J_c(y,z) \sin\left(\frac{2\pi}{\Phi_0} B_y t_B z + \varphi_0\right) \equiv J_c(y,z) \sin(kz + \varphi_0) \ , \tag{8}$$

where the critical current density J_c is in the most general form $J_c(y,z)$ with a spatial dependence. This result means, that the applied magnetic field leads to a sinusoidal current density in the junction along the z-axis. How many oscillation periods fit into the junction depends on the value of the magnetic flux Φ. This will be visualized in the following discussion.

2.1.2 Fraunhofer Pattern

To get the full picture of the current flow inside of the junction, it is reasonable to determine the total current by integrating over equation (8). The form of the current density J_s leads to a Fourier integral to obtain the *maximum total current* $I_s^m(\Phi)$ which is flux-dependent:

$$I_s^m(\Phi) = \left| \int_{-\infty}^{\infty} i_c(z) e^{\iota k z} dz \right| \ , \tag{9}$$

with $i_c(z)$ being the critical current density integrated over y. This expression can be solved assuming a spatially homogeneous $J_c(y,z)$, meaning that $i_c(z)$ is constant inside the junction and zero outside:

$$I_s^m(\Phi) = I_c \left| \frac{\sin(\frac{kL}{2})}{\frac{kL}{2}} \right| = I_c \left| \frac{\sin(\frac{\pi\Phi}{\Phi_0})}{\frac{\pi\Phi}{\Phi_0}} \right| . \tag{10}$$

This result represents the so-called *Fraunhofer pattern*, depicted in figure 4a. It is well known from

the narrow slit experiment in optics, where the intensity of the light behind the slit is described by this pattern. It should be no surprise that both experiments have this property, since the underlying physics is the same. The thin, rectangular shaped slit of length L is equivalent to the junction area. In the optical diffraction experiment the light intensity behind the slit is obtained through the Fourier transform of the transmission function $P_0(z)$, which is constant inside of the slit and zero outside. The corresponding quantity would be $i_c(z)$, which is plotted in 4a on the left.

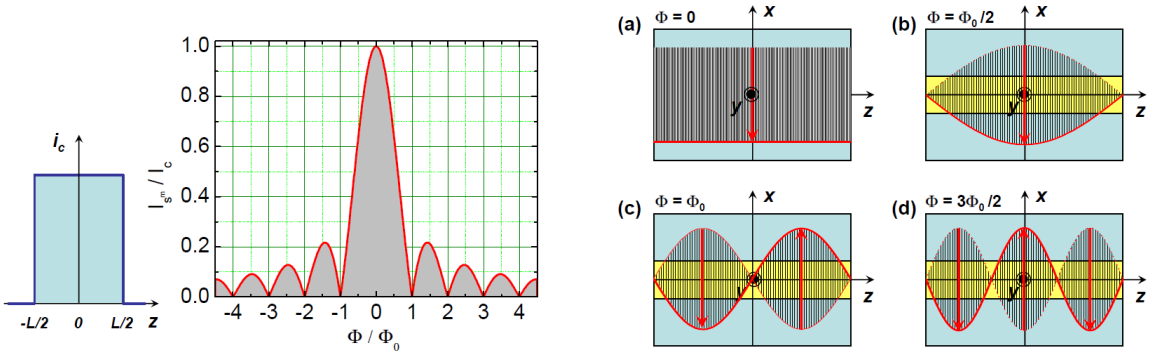

(a) (b)

Figure 4: Maximum total current $I_s^m(\Phi)$ given by the Fraunhofer pattern (a). Current distribution J_s visualized for different values of Φ (b).

It is important to note, that the modulation of $I_s^m(\Phi)$ is given by one flux quantum Φ_0. The current density distribution for different flux values is shown in figure 4b. As mentioned above, J_s oscillates along the z-axis with Φ defining the number of oscillations. For $\Phi = \Phi_0$ one total oscillation fits into the junction and the current direction goes from negative on the left side to positive on the right side. Consequently, the net current is zero, as can be verified through the Fraunhofer pattern. A vanishing current can be understood by the fact that the current on the right side of the junction will turn left at the top and join the downward flow and vice versa below the junction. This will form a closed current loop with one flux quantum trapped inside. The current drift to the side is reasonable, since shielding currents have to flow parallel to the junction area, preventing the magnetic field to penetrate the superconductor. This circular current flow is also known as a *Josephson vortex*.

2.2 Voltage State

So far only currents below the critical current were considered, such that no voltage drop occurs. This chapter will now cover the case of a non-zero voltage across the junction, hence the name *voltage state*.
There are two scenarios where a finite voltage can be obtained. The first involves increasing the current beyond the critical current I_c. Now the total current provided by the source cannot be carried by a supercurrent alone. This means that another type of current has to arise to keep the total current constant. This new current type has to be resistive and is therefore called the *normal current* I_N. Following Ohms law $U = RI$ a finite voltage will arise, as can be seen in figure 5a. Up to the critical current the curve remains at $V = 0$, afterwards it jumps onto the steep curve on the right side at $V \approx V_g$. This voltage defines the electric energy that is sufficient

to break up Cooper pairs, given by

$$V_g = \frac{\Delta_1(T) + \Delta_2(T)}{e} \tag{11}$$

Therefore, the steep slope represents Cooper pairs being broken up into quasiparticles, namely electron-hole pairs. As the voltage rises further, more and more quasiparticles are created until all Cooper pairs are broken up. From there on, the quasiparticles start to behave like normal conducting electrons and holes. Thus, the current continues following an ohmic dependence.

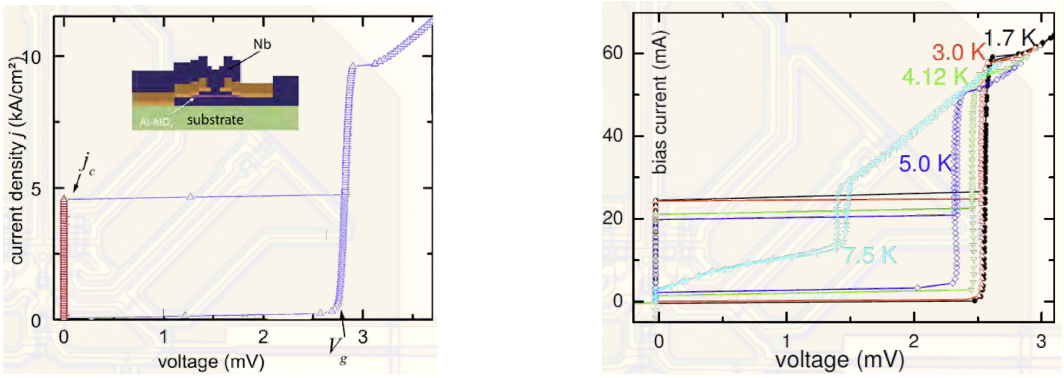

(a) (b)

Figure 5: Voltage dependence of the current density, transitioning from the zero voltage into the voltage state (a). IVCs for different temperatures (b).

The second mechanism that creates voltage is heat. Cooper pairs are restricted to low enough temperatures, depending on the material being used (Josephson junctions typically use Niobium). The plot in 5b shows how the *current-voltage-characteristic* (*IVC*) changes if the temperature is increased. For instance, at a relatively high temperature of 7.5 K the critical current is decreased significantly, as well as V_g. This is easily explained by the fact that thermal energy also breaks up Cooper pairs if it exceeds the sum of both gap energies $\Delta_1(T)$ and $\Delta_2(T)$. Also, $\Delta(T)$ decreases for increasing T, resulting in a lower V_g.

2.2.1 Basic Junction Equation

The presence of a finite voltage is not only associated with the normal current channel. A Josephson junction can be treated as a parallel plate capacitor with the electrodes representing the parallel plates and the insulator the dielectric material. The junction will therefore possess a capacitance C. If now the voltage is time-dependent, a displacement current I_D will flow in addition to the other current channels I_s and I_N.
Lastly, noise needs to be taken into account to obtain all the possible current types. Thermal noise leads to current fluctuations, which can be described by the *noise current* I_F. Figure 6 illustrates the equivalent circuit containing every current channel.

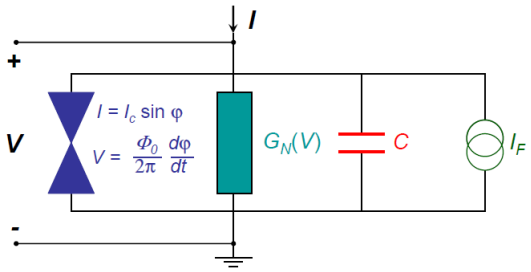

Figure 6: Circuit diagram showing all current channels which add up to the total current I. The cross-shaped symbol on the left represents a lumped (0-dimensional) Josephson junction.

The total current I, which is given by the current source, can then be expressed as

$$I = I_s + I_N + I_D + I_F = I_c \sin(\varphi) + \frac{1}{R(V)} \frac{\Phi_0}{2\pi} \frac{d\varphi}{dt} + C \frac{\Phi_0}{2\pi} \frac{d^2\varphi}{dt^2} + I_F \ . \tag{12}$$

This complex differential equation can only be solved numerically and is denoted as the *basic junction equation*. However, analytical solutions can be obtained by assuming a constant conductance $G(V) = G \quad (R(V) = R)$. Many important properties of Josephson junctions can be investigated by using this equation, such as *damping*. This is necessary to explain IVC curves that result from any current or voltage source that might be applied.

3 SQUIDs

Josephson junctions can be used for various applications. This chapter will focus on so-called *SQUIDs* (*superconducting quantum interference devices*), which are used in a wide range of fields. The high versatility of these devices stems from the ability to detect extremely small magnetic fluxes (order of 1 fT). In fact, SQUIDs are the most sensitive magnetometers to date. How they are built and why they work will be discussed in the following.

There are two common types of SQUIDs, namely the *dc-SQUID* and the *rf-SQUID*. The first operates with a dc current source and uses two Josephson junctions, while the latter has an ac current source and only needs one junction to operate. Nowadays most applications use dc-SQUIDs, which is why they will be the main focus from now on.
Figure 7 describes the general setup of a dc-SQUID. Two Josephson junctions are intersecting a superconducting loop and are considered to be identical. A dc current is sent through the loop, dividing into

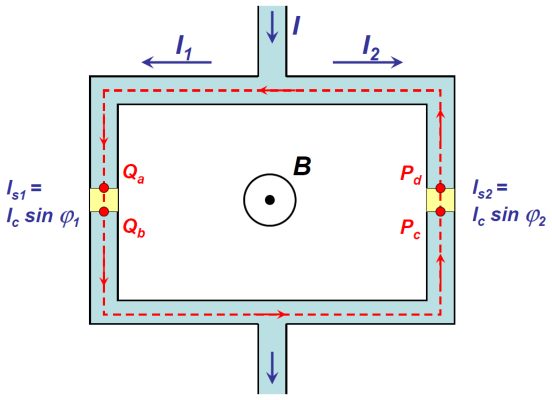

Figure 7: Schematic of a dc-SQUID.

I_1 and I_2. The loop is also threaded by a magnetic field $\mathbf{B}$, similar to the experiment with the superconducting cylinder. The reason for this geometry becomes clear when remembering how a single junction would react to a magnetic field. The behaviour of the supercurrent was addressed in chapter 2.1.2, where the flux dependence was shown in the form of the Fraunhofer pattern. The sensitivity of the junction would roughly be given by

$$\frac{I_s^m(\Phi)}{\Phi_0} = \frac{I_s^m(\Phi)}{B_0 t_B L} \ . \tag{13}$$

Evidently, a larger area threaded by the B-field allows for smaller fields. A single junction would not be suited to measure small fluxes, for the effective area would be to small. SQUIDs on the contrary, have a large area formed by the superconducting loop. It turns out, that the current behaviour is comparable to that of a single junction. Therefore, it can be regarded as a single junction with a large L and t_B.
This allows for measuring fluxes of the order of fT, which is well below conventional coil magnetometers.

3.1 Voltage State of a dc-SQUID

SQUIDs are typically operated in the voltage state. An expression for the voltage can be obtained by assuming negligible screening currents (small inductance L of the loop) and strong damping (negligible junction capacitance C). Then, the total current has the same form as for a single Josephson junction (see eq. (12)), now with the critical current being flux-dependent. The voltage of a single overdamped junction can be derived to

$$\langle V(t) \rangle = IR\sqrt{1 - \left(\frac{I_c}{I}\right)^2} \ . \tag{14}$$

Due to the equivalence of the single junction and the SQUID regarding the current, eq. (14) can be used to obtain

$$\langle V(t) \rangle = IR\sqrt{1 - \left(\frac{I_s^m(\Phi_{ext})}{I}\right)^2} = IR\sqrt{1 - \left[\frac{2I_c}{I}\cos\left(\pi\frac{\Phi_{ext}}{\Phi_0}\right)\right]^2} \ , \tag{15}$$

with $I_s^m(\Phi_{ext}) = 2I_c\cos(\pi\frac{\Phi_{ext}}{\Phi_0})$.

This important result is visualized in figure 8. The 3D plot (8a) shows the dependence of $\langle V(t) \rangle$ from I and Φ. Figure 8b represents intersections of the 3D plot in different planes. For instance, the flux-modulated voltage for several current values ranging from $I = 2I_c$ to $I = 4I_c$ is depicted in plot (c) from figure 8b. As mentioned before, SQUIDs are used to detect small magnetic fluxes. This is achieved by measuring the flux-dependent voltage, where a strong modulation means a large voltage change δV is obtained from a small flux change $\delta\Phi$. The bottom curve is thus preferable where the current is roughly $2I_c$. Evidently, SQUIDs are operated at the so-called *working point*, which marks the steepest point in the V-Φ curve.

3.2 dc-SQUID readout

The question is now how such a measurement can be realized with a real SQUID including additional electronic components. In general the setup is composed of three parts: A coil (antenna)

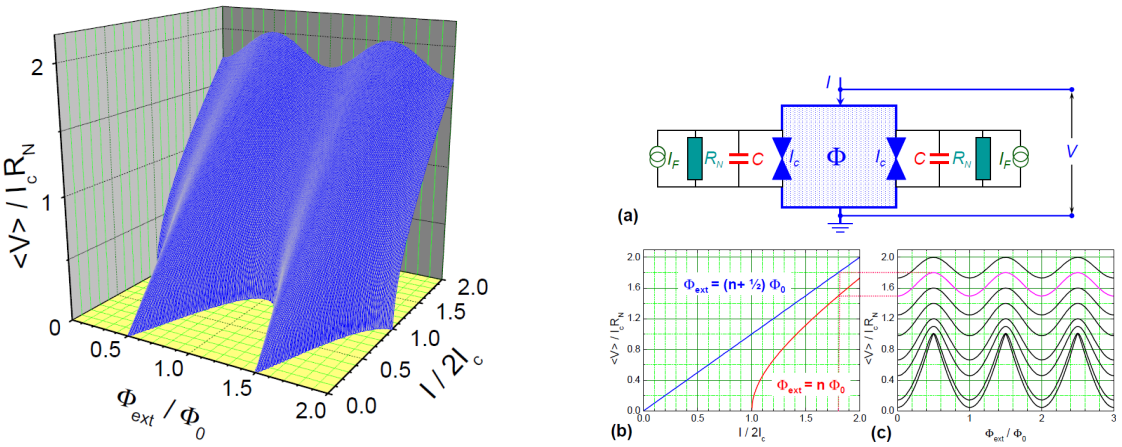

(a) (b)

Figure 8: 3D plot of $\langle V \rangle$ (a). Current and flux dependence of the voltage (b).

is used to transfer the signal of interest into the SQUID. This is achieved by placing the coil on top of the SQUID loop such that it is optimally coupled. The second part consists of the SQUID embedded in very low temperatures, which produces a voltage due to the flux threading the loop. This voltage signal is then brought to room temperature electronics, which represents the rest of the setup.

Two important technical aspects need to be addressed in order to obtain meaningful results. The first is finding a solution for the coupling of the external flux one wants to measure into the SQUID. Here, the ideal setup was found to be the *washer type* geometry as depicted in figure 9. The blue rectangular shape represents the superconducting loop of the SQUID. The input coil (red) is placed on top of the loop, separated by a thin insulating layer to avoid a shorted circuit. A realistic depiction with a length scale is shown on the right.

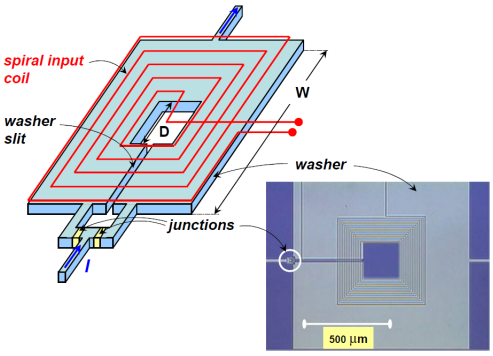

Figure 9: Washer-type dc-SQUID.

Secondly, the signal needs to be linearized. As seen above, the flux dependence of the voltage exhibits a modulation with Φ_0. A voltage change δV will therefore correspond to ambiguous flux values. This is why it is desirable to maintain the measurement close to the working point, where the dependence is approx. linear and also the so-called *transfer coefficient*

$$H := \left| \frac{\partial V}{\partial \Phi_{ext}} \right| \tag{16}$$

is maximal. This is solved by the *flux-locked loop* method, shown in figure 10. Here, the SQUID operates as a null-detector using a feedback loop. The voltage produced by a small flux change

is transmitted to a room temperature amplifier to obtain a larger signal. The voltage at the working point V_b is being compared to the signal, such that amplification only appears for $V \neq V_b$. An integrator will then produce a rising voltage over time, as long as the input is finite. V_{OUT} is now connected to a feedback resistor R_{FB}, followed by a feedback coil. The latter is coupled to the SQUID, such that it produces a flux with opposite polarisation with respect to the input flux. The rising voltage will lead to a rising current in the feedback coil, resulting in a flux that eventually cancels out the initial one. At this point, the SQUID is set back to V_b and V_{OUT} becomes 0. This way the SQUID will remain close to the working point and the signal is linearized.

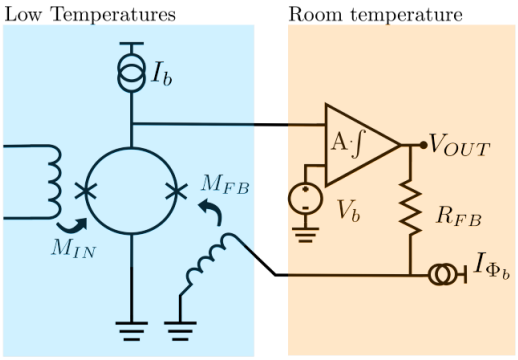

Figure 10: Circuit of a flux-locked loop operation.

3.3 SQUID applications

SQUIDs are extremely versatile and used in many fields of research. This also stems from the fact that depending on the antenna, many physical quantities can be transformed into magnetic flux such as magnetic field gradient, current or voltage. Some of the most important applications will be briefly discussed in the following:

Biology/Medicine: SQUIDs provide a significant contribution to medical research. The most prominent example here is magnetoencephalography (MEG), which describes the process of brain activity mapping. Many neurons transmitting electrical signals are able to produce tiny magnetic fields in the order of 100 fT, which is above detection threshold. For this measurement, an array of SQUIDs are used around the patients head to investigate brain activity with high spatial resolution.
Other biomagnetism applications include magnetocardiography (heart measurements), magnetic marker monitoring, MRI and many more.
Geophysics: Magnetized rock samples can be analyzed non-destructively by measuring the field distribution they exhibit, such that conclusions about possible materials inside can be made.
Also, a large social and economic interest lies in mineral exploration. Materials below Earths surface can influence Earths magnetic field, such that air-borne SQUIDs (attached to a plane or helicopter) can be used as gradiometers to detect them. Similarly, SQUIDs became an essential tool in archeology.
Particle Physics Some particle detectors also take advantage of the high sensibility SQUIDs provide. An example are so-called *metallic magnetic calorimeters* (MMC). They allow for detection of single photons by using an absorber that heats up by absorbing the particle. An attached paramagnet, surrounded by an external B-field, heats up as well causing its susceptibility to rise. The small change in magnetization will then result in a small flux change which is measurable with SQUIDs. MMCs are used for example to search for cold dark matter.

There are numerous other examples where superconducting quantum devices like Josephson junctions or SQUIDs play an important role. They include Astronomy, quantum computing (qubits), thermometry, displacement/gravity/motion sensors, etc.

Literature

- Groß, Marx; *Applied Superconductivity: Josephson Effect and Superconducting Electronics.* Walther-Meissner-Institut (Manuscript to the lecture during WS 2003/04)
- Stolz, Schmelz et. al.; *Superconducting Sensors and Methods in Geophysical Applications.* Superconductor Science and Technology, Volume 34, Number 3.
- Behrend; *Assembly and Characterization of a SQUID Amplifier Module for IAXO and Automation of SQUID Tuning.* Bachelor Thesis at Kirchhoff Institute for Physics in Heidelberg (2021)
- Stolz, Zakosarenko et. al.; *Magnetic full-tensor SQUID gradiometer system for geophysical applications.* The Leading Edge 25: 178-180
- https://en.wikipedia.org/wiki/SQUID
- https://en.wikipedia.org/wiki/Magnetoencephalography